

Original Research Article

USE OF ARTIFICIAL NEURAL NETWORK AND RESPONSE SURFACE METHODOLOGY FOR MODELLING AND OPTIMIZING THE REMOVAL OF Pb(II) ONTO SHARP SAND

ABSTRACT

Aims: This study was aimed at using sharp sand as an adsorbent to optimize the removal of Enyigba from simulated water and water obtained from Enyigba River

Study design: Adsorption experiment was designed using Response Surface Methodology (RSM). Artificial Neural Network (ANN) was also used to predict % Enyigba removal.

Place and Duration of Study: Department Of Pure and Industrial Chemistry, Nnamdi Azikiwe University, Awka, June 2012 to June 2023

Methodology: Sharp sand was modified with salicylic acid, noted as SSM and then characterized. Experiments were carried out by varying four adsorption factors namely concentration, time, pH and temperature. Adsorption experiments were also done for equilibrium isotherm, kinetics and thermodynamic studies.

Results: The modified sharp sand showed a high percent of silicon. RSM and ANN predicted the sorption of Enyigba well with R^2 values > 0.9 . The optimal values for concentration, time, pH and temperature are 0.0125mg/l, 100sec, 2, 20°C respectively. Langmuir isotherm gave the better fit and adsorption was endothermic with positive ΔH . Adsorption followed second order kinetics. FTIR analysis showed the presence of functional groups that were responsible for adsorption. Enyigba River water is slightly polluted with lead ions with concentration higher than WHO standard.

Conclusion: The adsorbent was able to remove over 70% of the metal ions from both the simulated and Enyigba River water.

Keywords: [Adsorption, Neural Network, Kinetics, Optimization]

1. INTRODUCTION

Enyigba is a rural community in the south-eastern part of Nigeria which is 14 km southeast of Abakaliki with its surrounding villages as Ameka, Ameri and Ohankwu. It lies between latitudes 6°07'N and 6°12'N and longitudes 8°05'E and 8°10'E in the derived savannah vegetation. The population of Enyigba Community (suburb of Abakaliki) is estimated to be 8,000 from 79,280 population of Abakakili [1]. The open cast mining activities in Enyigba compounds the problem of water scarcity in the region as a result of leakage of heavy metals that pollute the limited water resources [2]. Open cast mining is a mining process that leads to removal of vegetation and heavy equipment and hard implements are employed to mine a target mineral [3],[4] and as a result, pits and dumps are created leading to land degradation [5a]. The presence of Pb-Zn-Fe ore mine in Enyigba region has made mining a regular practice in that region both legally and illegally. The proximity of Enyigba River to the mining vicinity suggests that the stream might be contaminated by toxic elements from tailings arising from mining activities through wind and water within the vicinity of the mining area [5b]. Heavy metals are a class of metallic elements with density exceeding 5.0g/mL, which are abundant in earth's crust [6]. They are very toxic and non-biodegradable materials that bioaccumulate, causing health problems and essentially cause degradation of biodiversity in the environment [7]. They are soluble in water by dissolution. The impact of heavy metals in water bodies has created vast environmental pollutions [8]. Consequently, urbanization and industrialization produce and release heavy metals that reach the land and water on the surface and percolate into the soil [6]. The concentration of these heavy

metals exceed limit thereby causing severe health risk to biological organisms [8]. Heavy metals commonly found in water include; Copper (Cu), Zinc (Zn), Gold (Au), Mercury (Hg), Cadmium (Cd), Iron (Fe), Nickel (Ni), Tin (Sn), Arsenic (As), Selenium (Se), Molybdenum (Mo), Cobalt (Co), Manganese (Mn) and Aluminum (Al) [9]. However, at higher concentrations they can lead to poisoning. Heavy metal poisoning could result, for instance, from drinking water contamination (e.g. lead pipes), high ambient air concentrations near emission sources, or intake via the food chain. When dynamite used in opencast mining explodes, some particles from the mine find their way into the stream and contaminate it, making it unsafe for use; hence the need for the stream water to be treated with easily sourced adsorbents. This study was aimed at using sharp sand as an adsorbent to optimize the removal of Pb^{2+} from simulated water and water obtained from Enyigba stream in Ebonyi State.

2. MATERIAL AND METHODS

2.1 Materials

The sharp sand was obtained from a construction site in Awka. It was washed with distilled water to remove impurities and dried in a hot air oven at 110°C for at least 12 hours. All the chemicals used in this work were of analytical reagent grade purchased from Sigma Aldrich and were used without any further purification. All the glass wares used were washed and rinsed several times.

2.2 Modification and characterization of the modified sharp sand

The modification of sharp sand with salicylic acid was done by dissolving 120g of salicylic acid in water, followed by addition of little quantity of acetone to enhance the dissolution of the acid. 1L of the salicylic acid solution was added to the adsorbent and mixed thoroughly. This was then allowed to stay for 24hours for proper equilibration. It was filtered and the residue was oven dried at 300 °C for one hour. This was labelled as SSM. The morphology of the adsorbents was determined using the Scanning Electron Microscope (SEM). The SEM was used to examine the surface morphology and the porous nature of the material responsible for adsorption of metal ions. The functional groups present in the adsorbents were determined by the Fourier-Transform Infrared (FT-IR). The FT-IR analysis allowed spectrophotometric observation of adsorbent surface in the range 400-4000 cm^{-1} and served as a direct means for the identification of the functional groups on the surface

2.3 Design of experiment

Response surface methodology (RSM) of Minitab 17 software was used to design the experiments. Central composite design (CCD) of RSM was applied to assess the effects of main factors at five different levels. Additionally, analysis of variance (ANOVA) was used to determine the significance of model and model parameters.

The CCD method is appropriate for fitting a quadratic surface and was used to optimize the parameters with a minimum number of experiments, as well as to analyze the interaction between the parameters.

Experimental data were subjected to 2nd order polynomial regression analysis using the least square regression model containing 4 linear, 4 quadratic and 6 interaction terms.

$$Y = b_0 + b_1A + b_2B + b_3C + b_4D + b_{11}A^2 + b_{22}B^2 + b_{33}C^2 + b_{44}D^2 + b_{12}AB + b_{13}AC + b_{14}AD + b_{23}BC + b_{24}BD + b_{34}CD$$

Y is the response (% removal), b's are constant regression coefficients, A, B, C and D are initial concentration (mg/L), contact time (min), pH, and solution temperature (°C) respectively. Statistical significance of the variables was determined by p-values. The lack of fit is performed by comparing the variability of the current model residuals to the variability between observations at replicate settings of the factors. The lack of fit is designed to determine whether the selected model is adequate to describe the observed data, or whether a more complicated model should be used.

Experimental range and levels of the independent variables for Pb^{2+} ion adsorption are shown in table 1. The design matrix is shown in table 2

Table 1: Experimental range and levels of the independent variables

Variables	Code	Unit	Coded variable levels				
			- α	-1	0	+1	+ α
Concentration	A	mg/l	0.0125	0.05	0.0875	0.125	0.1625
Time	B	min	20	40	60	80	100
pH	C	-----	2	4	6	8	10
Temperature	D	°C	20	40	60	80	100

2.4 Optimization of Chromate Reduction by Artificial Neural Network (ANN).

In this study, neural network of SPSS mathematical software was used for simulation. The same experimental data which was used for the RSM design were also employed in designing the artificial neural network. The input variables were concentration, time, pH and temperature. The corresponding % removal was used as a target. The data were randomly divided into three groups, 70% in the training set, 15% in the hold out set and 15% in the test set. Automatic architecture with minimum and maximum number of units of 1 and 50 was selected. Hyperbolic tangent at hidden layer and identity function at output layer were used. Batch training function and optimized algorithm of scaled conjugate gradient were

selected for the network. Batch training uses information from all records in the training dataset and is often preferred because it directly minimizes the total error [10]. All variables and response were normalized between 0 and 1 for the reduction of network error and higher homogeneous results. The normalization equation applied is as follows:

$$y_n = \frac{y_a - y_{min}}{y_{max} - y_{min}} \quad 2$$

y_n , y_a , y_{min} and y_{max} are normalized value, actual value, minimum value, and maximum value, respectively. The architecture of the network is shown in fig 1

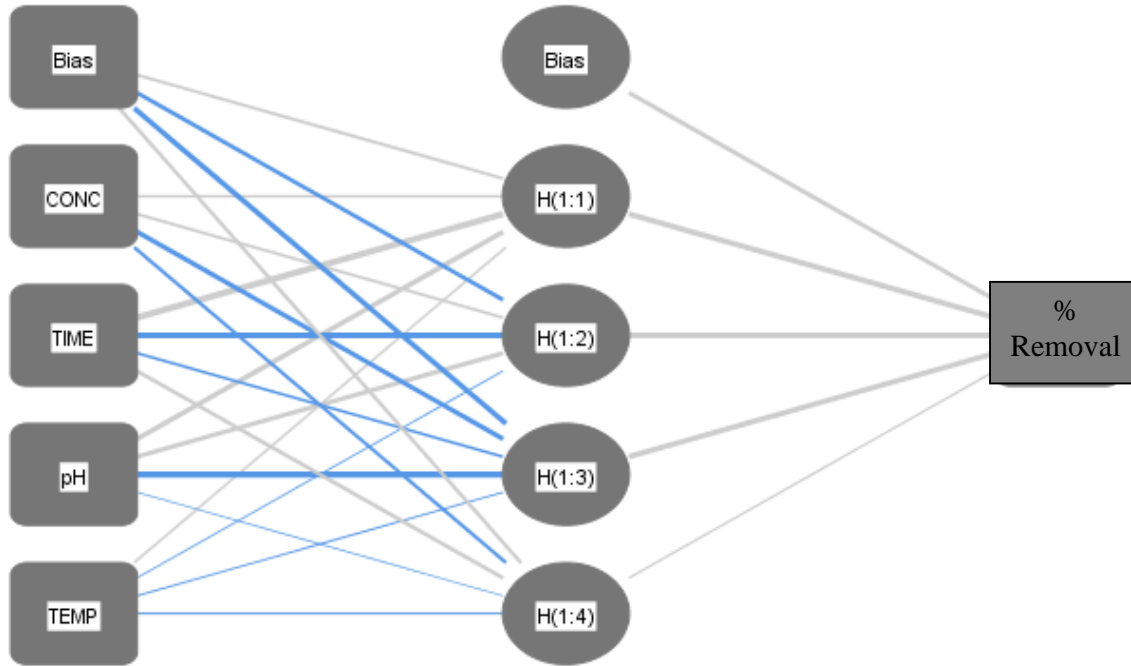


Fig. 1: Artificial neural network architecture

2.5. Metal ions adsorption experiments

A standard solution of 1000 mg/l Pb^{2+} was prepared from its nitrate salt. The different solutions used throughout the study were prepared from the serial dilution of the standard solution. For equilibrium isotherm studies, experiments were carried out with concentration varied in the range 0.01mol/dm^3 - 0.0025mol/dm^3

Experiments for kinetics of adsorption were done in the time range 20 and 100 min while those for thermodynamics studies were carried out in the temperature range of 25 and 100°C in a thermostated bath. In each case, 60ml of the required Pb^{2+} ion solution and 5 g of SSM were used. Each mixture of metal ion solution and adsorbent was thoroughly stirred using a magnetic stirrer and allowed to stand for the necessary time. Afterwards the mixture was filtered and the filtrate analyzed for Pb^{2+} ion removal using atomic absorption spectrophotometer.

2.5.1. Removal of Pb^{2+} ions content of the water sample from Enyigba

Optimal values of experimental factors (pH, time, concentration, temperature) were finally employed to remove Pb^{2+} ions from Enyigba River water sample. Water sample was analyzed to determine the concentration of Pb^{2+} ion before and after treating the water sample with SSM.

The amount of the metal ion adsorbed per gram of adsorbent was obtained by using equation:

$$q_e = \left(\frac{C_o - C_e}{m} \right) * v \quad 3$$

The percentage removal of the metal ions Pb^{2+} , was calculated using the equation:

$$\text{percentage removal} = \left(\frac{C_o - C_e}{m} \right) * 100 \quad 4$$

q_e is the amount in mg/g adsorbed, C_o and C_e are the initial and equilibrium concentrations of metal ions in (mg/l), v is the volume in litres of the metal ion solution used and m is the weight of the adsorbent in g.

2.6. ISOTHERM STUDY

The equilibrium characteristics of this adsorption study were described through Langmuir and Freundlich isotherm models. The Langmuir adsorption isotherm model assumes that adsorption takes place at specific homogeneous sites within the adsorbent, and it has been used successfully for many adsorption processes of monolayer adsorption [11]

The Langmuir equation is expressed by the following relation

$$q_e = \frac{q_m k_a c_e}{1 + K_L C_e} \quad 5$$

The linearized form of Langmuir isotherm that can be written in two different forms; Langmuir-1 isotherm model

$$\frac{C_e}{q_e} = \frac{C_e}{q_m} + \frac{1}{K_L q_m} \quad 6$$

From the slope and intercept of the plot between $\frac{C_e}{q_e}$ vs C_e , q_m and K_L are obtained respectively. Langmuir-2 isotherm model

$$\frac{1}{q_e} = \frac{1}{K_L q_m C_e} + \frac{1}{q_m} \quad 7$$

In this form q_m and K_a are obtained from the plot of $\frac{1}{q_e}$ vs $\frac{1}{C_e}$

q_m (mg/g) is the maximum % removal and K_L (L/mg) is the Langmuir constants related to rate of adsorption. The essential characteristics of Langmuir model described by the dimensionless separation factor R_L is given as

$$R_L = \frac{1}{1 + K_L C_o} \quad 8$$

R_L values indicate whether the adsorption is unfavourable ($R_L > 1$), linear ($R_L = 1$), favourable ($0 < R < 1$), or irreversible ($R_L = 0$)

The Freundlich adsorption isotherm model considers a heterogeneous adsorption surface that has unequal available sites with different energies of adsorption. The Freundlich adsorption isotherm model is represented as follows [12].

$$q_e = K_f C_e^{\frac{1}{n}} \quad 9$$

The linearized form of Freundlich can be expressed as;

$$\ln q_e = \ln K_f + \frac{1}{n} (\ln C_e) \quad 10$$

K_F and n are Freundlich constants denoting adsorption capacity and intensity of adsorption respectively. Generally, $n > 1$ suggests favourable adsorption. It has also been used to evaluate whether the adsorption process is physical ($n > 1$), chemical ($n < 1$) or linear ($n = 1$). The plot of $\ln q_e$ vs $\ln C_e$ is employed to determine the K_F and n from intercept and slope respectively.

Generally the value of the linear regression coefficient of determination R^2 gives an indication as to which model gives the best-fit.

2.7. Kinetics of adsorption

The pseudo first order kinetic model equation is used in explaining the adsorption rate based on the adsorption capacity and is generally expressed as follows [13]:

$$\ln(q_e - q_t) = \ln q_e - k_1 t \quad 11$$

Where q_e is the amount of adsorbate adsorbed at equilibrium, (mg/g), q_t is the amount of solute adsorb per unit weight of adsorbent at time, (mg/g), k_1 is the rate constant of pseudo-first order sorption (mg/l/h).

A plot of $\ln(q_e - q_t)$ versus t gives a straight line with slope of k_1 and intercept of $\ln q_e$.

From the intercept, q_e theoretical is obtained.

The pseudo-second-order equation can be expressed as:

$$(q_e - q_t) = \frac{1}{q_e} + k_2 t \quad 12$$

where k_2 in (g/mg min) is the pseudo second order rate constant. The above equation can be rearranged to obtain its linear form as:

$$\frac{t}{q_t} = \frac{1}{k_2 q_e^2} + \frac{1}{q_e} t \quad 13$$

A plot of t/q_t against t gives a straight line with slope of t/q_e and intercept of $1/k_2 q_e^2$

The intra-particle diffusion equation is given as:

$$q_t = k_i t^{1/2} + C \quad 14$$

Where q_t is the amount of solute on the surface of the sorbent at time t (mg/g) and k_i is the intraparticle diffusion rate constant (mg/g min^{1/2}). When intraparticle diffusion alone is the rate limiting step, then the plot of q_t versus $t^{1/2}$ passes through the origin. When film diffusion is also taking place then the intercept is C , which gives the idea on the thickness of the boundary layer [14].

3. RESULTS AND DISCUSSION

Biochemical analysis of Enyigba River was done, results are shown in table 2. The colour, turbidity, TSS, coliform and lead content were above the WHO permissible limit. This shows that the River is contaminated

Table 2: Biochemical analysis of Enyigba River

PARAMETER	MEASURED VALUE	WHO[15]
pH	7.32	6.5-8.5
Colour(pcu)	149	5
Turbidity(NTU)	11.36	0.5
BOD mg/l	1.7	5
Nitrates mg/l	18.93	50
Coliform cfu/ml	65	0
Lead mg/l	0.0218	0.01

Adsorbent characterization

The FTIR spectrum of SSM is shown in Fig 2. Several Si-Si-OH or Al-Al-OH bands were observed at 3554.14 to 3182.67 [17]. Intense bands were observed at 2928.84, 2702.55, 2443.40 and 1979.61 and they indicate high presence of C-H stretch, OH stretch and vibrations of cumulative C= bonds or aromatic C-H respectively [16]. The absorption at 1633.41 represents COO- symmetric stretching vibrations This has also been observed by [17]. The absorption between 732.52 - 872.79 cm^{-1} The peaks detected at 786 and 673 cm^{-1} , as well as 789 and 647 cm^{-1} , were ascribed to the valence vibrations of the Si-O bonds of quartz [18]

The SEM-EDX result in table 3 shows the silicon as the major component in the adsorbent. Modification with salicylic acid reduced the silicon content of the adsorbent while other elements like nitrogen, oxygen and aluminum increased slightly. The SEM morphology is shown in fig 3, the EDX graph is shown in fig 4. The porous nature of the adsorbent was revealed by the SEM image with an increase in surface porosity after modification. The increase in the porous nature of SSM indicates that adsorption would be enhanced [19].

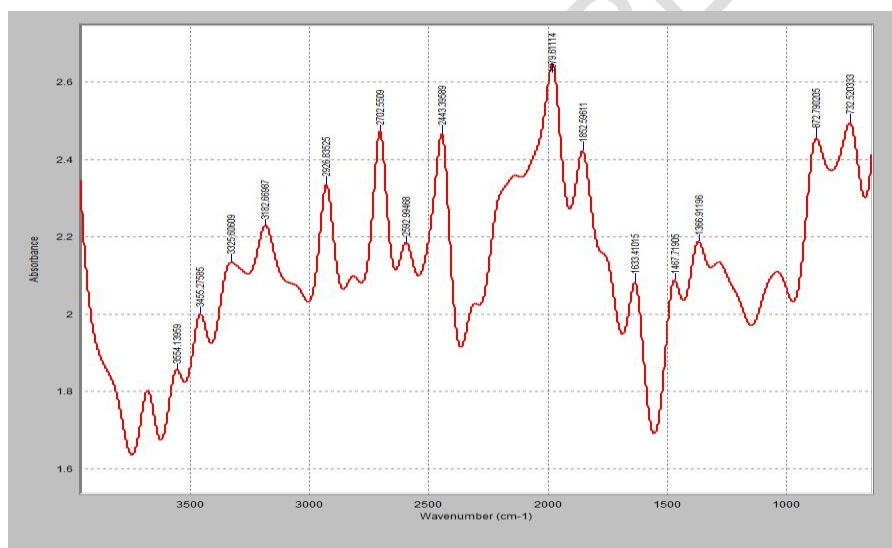


Fig 2: Fourier Transform Infrared Spectrum of SSM

Table 3: SEM-EDX analysis

Element	Atomic weight
Nitrogen	11.73
Oxygen	4.94
Aluminium	3.89
Silicon	79.44

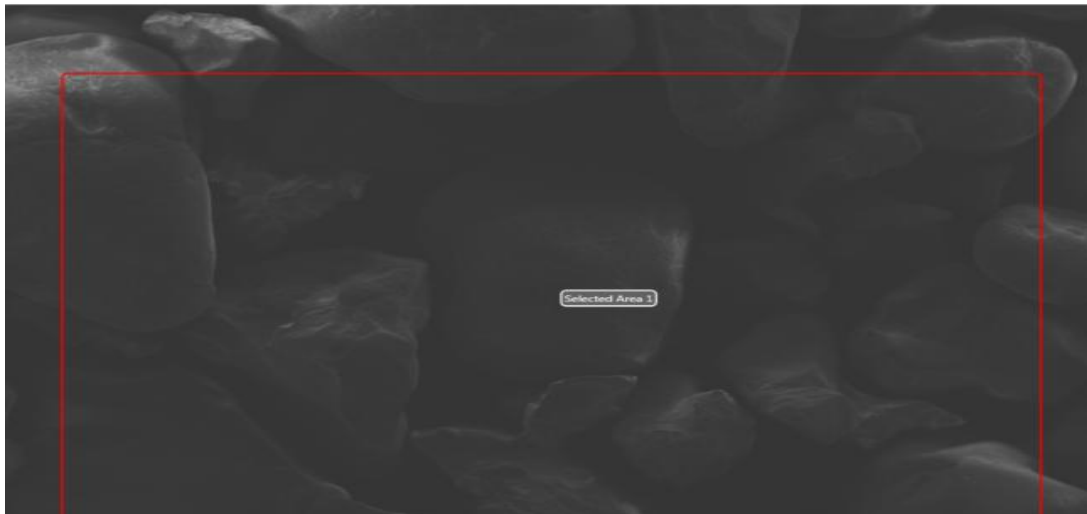


Fig 3: SEM morphology of the salicylic modified sharp sand (SSM)

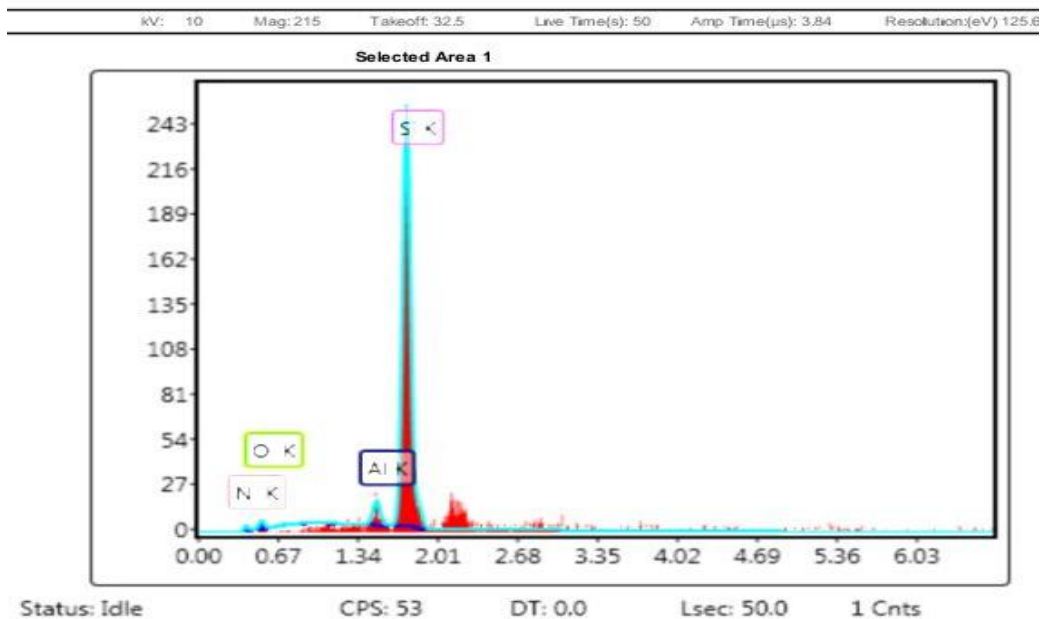


Fig 4: EDX graph of the salicylic modified sharp sand (SSM)

Optimization process using RSM and ANN

The experimental and predicted adsorption capacities results for the adsorbents are shown in table 4. The range of adsorption is 63.27-85.86. In all cases, over 60% of the metal ions was removed using the prepared adsorbent. This shows good adsorption efficiency. The plots of RSM and ANN predicted adsorption capacities against experimental % removal are shown in fig 4. The predictions were good with R^2 values > 0.9

Table 4: Experimental design matrix using central composite

Conc mg/l	Time (min)	pH	Temp (°C)	% Removal		
				EXPT	RSM	ANN
-1	1	-1	-1	95.62	95.32	90.64
1	1	1	1	65.4	65.44	68.15
-1	-1	-1	1	72.89	71.22	74.7

0	- α	0	0	63.87	63.4	70.58
-1	1	-1	1	79.09	78.89	90.21
0	0	0	0	67.96	68.7	66.35
0	0	0	0	67.96	68.7	66.35
1	-1	-1	1	69.87	71.22	66.3
-1	1	1	-1	63.14	63.37	67.37
0	0	0	- α	64.69	63.89	64.07
1	-1	1	1	66.5	66.56	67.69
0	0	0	+ α	65.77	66.24	67.47
1	-1	-1	-1	74.66	73.81	71.52
0	0	0	0	66.4	67.64	66.35
0	+ α	0	0	66.99	67.13	66.54
- α	0	0	0	69.58	67.64	76.63
1	-1	1	-1	68.71	68.47	67.17
0	0	0	0	67.9	67.64	66.35
-1	1	1	1	75.82	74.84	66.91
1	1	-1	-1	68.57	68.87	70.85
-1	-1	1	1	66.28	66.56	67.64
-1	-1	-1	-1	71.67	73.81	77.56
1	1	-1	1	67.34	67.89	68.91
+ α	0	0	0	66.55	67.11	76.51
1	1	1	-1	67.87	68.31	69.39
0	0	2	0	67.51	67.03	65.07
0	0	0	0	67.9	67.11	66.35
0	0	0	0	67.9	67.11	66.35
0	0	10	0	93.58	93.73	92.97
-1	-1	1	-1	72.41	72.64	68.05
0	0	0	0	66.96	67.11	66.35

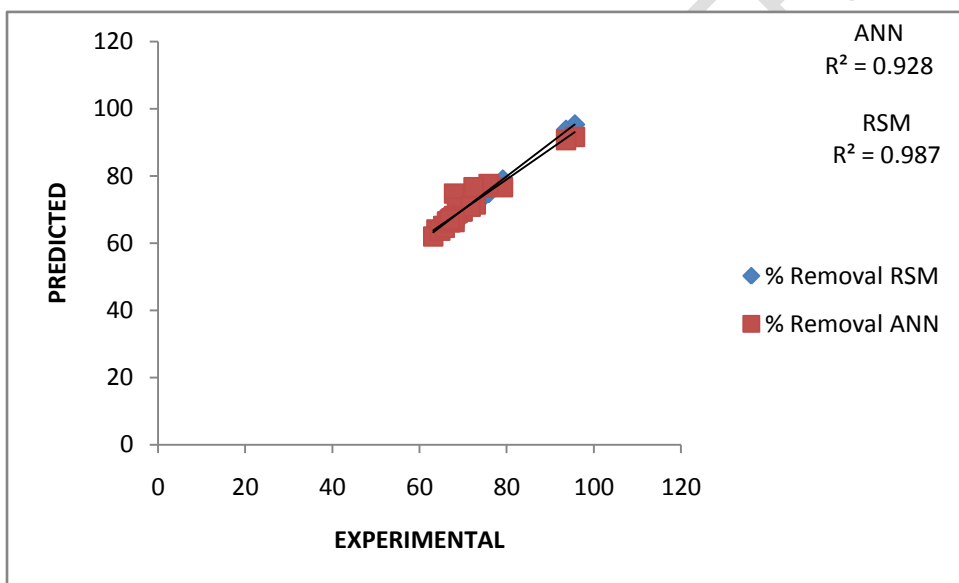


Fig. 5: Relationship between predicted and experimental data for Pb (II) removal

Statistical analysis

The adequacy of the model was further verified through analysis of variance (ANOVA). Table 5 shows the ANOVA result for the quadratic model for Enyigba percentage removal. The model terms with value of $P < 0.05$ are considered as significant [20]. From the table, the model F-value is 86.59 at $P < 0.05$, justifying the model's significance that at least one of the terms in the model has an impact on the mean response (% removal). This is also seen in the percentage contribution (98.7) of the model in describing the process of adsorption. This implies that the mode variables could account for 98% variation in the % removal; while 1.3% variation was due to error in the model. The model is further broken into the different orders of terms: linear, square, and interaction. All four factors varied in the adsorption study have

p- values < 0.05. This indicates that their linear effects on the adsorption process were quite significant. Squared terms are used to evaluate whether or not there is curvature in the response surface. The p-value of 0.000 for the squared effects is less than 0.05. Therefore, there is significant evidence of a quadratic effect in which adsorption surface was curved. The individual p-values for pH*pH and Temperature*Temperature are 0.000 and 0.012 respectively, indicating that the relationships between pH and adsorption and temperature and adsorption follow a curved line. The p-values for the concentration *pH, concentration * temperature, time * temperature and pH * temperature interactions are less than 0.05. Therefore, there are a significant interaction effects: the effect of concentration on percentage removal depends on the pH and temperature and that of temperature depends on time and pH. From the statistical results obtained, it can be seen that the models were suitable in predicting Enyigba removal within the range of the studied variables.

The final empirical model regression equation of adsorption is given below:

$$\% \text{ Removal} = 120.2 - 440 A + 0.577 B - 14.64 C - 0.143 D + 849 A^2 - 0.00022 B^2 + 0.953 C^2 - 0.00098 D^2 - 2.50 AB + 52.2 AC + 0.92 AD - 0.0472 BC + 0.00021 BD + 0.0222 CD \quad 15$$

The synergetic and antagonistic effects of the respective variables were informed by the positive and negative signs before the terms. The appearance of a single variable in a term signified a linear effect; two variables imply an interactive effect and a second order term of variable appearance indicate the quadratic effect [21].

The regression equation shows that adsorption had indirect relationship with concentration, pH, and temperature but had a direct relationship with time. The quadratic effect of concentration and pH and the interactive effect of concentration and pH, concentration and temperature, time and temperature, pH and temperature had a direct relationship with adsorption whereas the quadratic effect of time, temperature and the interactive effect of concentration and time, time and pH had indirect effect on adsorption.

Table 5 The ANOVA for response surface quadratic model of Pb (II) by SSM

Source	DF	Seq SS	% Contribution	Adj SS	Adj MS	F-Value	P-Value
Model	14	1608.99	98.70	1608.99	114.928	86.59	0.000
Linear	4	102.1	6.26	57.48	14.369	10.83	0.000
A	1	55.33	3.39	7.39	7.39	5.57	0.031
B	1	28.38	1.74	10.83	10.828	8.16	0.011
C	1	0.92	0.06	15.24	15.238	11.48	0.004
D	1	17.47	1.07	6.24	6.237	4.7	0.046
Square	4	646.72	39.67	324.28	81.071	61.08	0.000
A ²	1	233.02	14.29	1.15	1.155	0.87	0.365
B ²	1	19.07	1.17	5.6	5.599	4.22	0.057
C ²	1	394.28	24.19	299.42	299.419	225.6	0.000
D ²	1	0.35	0.02	10.71	10.713	8.07	0.012
2-Way Interaction	6	860.17	52.76	860.17	143.361	108.02	0.000
AB	1	39.19	2.40	2.84	2.835	2.14	0.163
AC	1	605.57	37.15	748.67	748.671	564.09	0.000
AD	1	97.14	5.96	85.78	85.776	64.63	0.000
BC	1	12.9	0.79	2.81	2.815	2.12	0.165
BD	1	87.03	5.34	94.9	94.904	71.51	0.000
CD	1	18.34	1.12	18.34	18.337	13.82	0.002
Error	16	21.24	1.30	21.24	1.327		
Lack-of-Fit	8	5.9	0.36	5.9	0.738	0.39	0.901
Pure Error	8	15.33	0.94	15.33	1.916		
Total	30	1630.22	100.00				

Optimum conditions for adsorption

The optimum conditions for adsorption are shown below in table 6. D* is Desirability, % R* is percentage response of adsorption, CI is confidence interval, PI is predicted interval. A look at the table shows that predicted response fall within the boundaries of CI and PI. This is acceptable and excellent because the value is above target value. The desirability of 1 indicates that the responses achieved their ideal setting.

Table 6: Values of adsorption variables for optimal adsorption

Goal	Lower	Target	Variable Prediction				% R*	SE Fit	D*	95% CI	95% PI
			A	B	C	D					
Max	66.28	99.58	0.0125	100	2	20	131.8	23.7	1	(81.7, 182.0)	(78.8, 184.8)

Isotherm studies

The equilibrium isotherm model parameters for the adsorption of Enyigba ions unto the adsorbent are shown in table 7, while the isotherm plots are shown in figs. 5 and 6

Table 7: Isotherm parameters

Model	Parameter	
Langmuir	R ²	0.916
	q _m (mg/g)	0.571
	K _L	0.008
Freundlich	R _L	0.9998
	R ²	0.905
	n	1.512
	K _F	0.0005

From the table, coefficient of determination (R²) were above 0.9 for Langmuir and Freundlich, isotherms indicating a good fit of both models. It shows that the process of Enyigba removal was a complex one. The isotherms could account for over 90% of the variations that occurred in the sorption process. From the table, the values of n was greater than 1. This implies that the adsorption process was physical in nature [22]. R_L value was less than 1 and shows a favourable process [23].

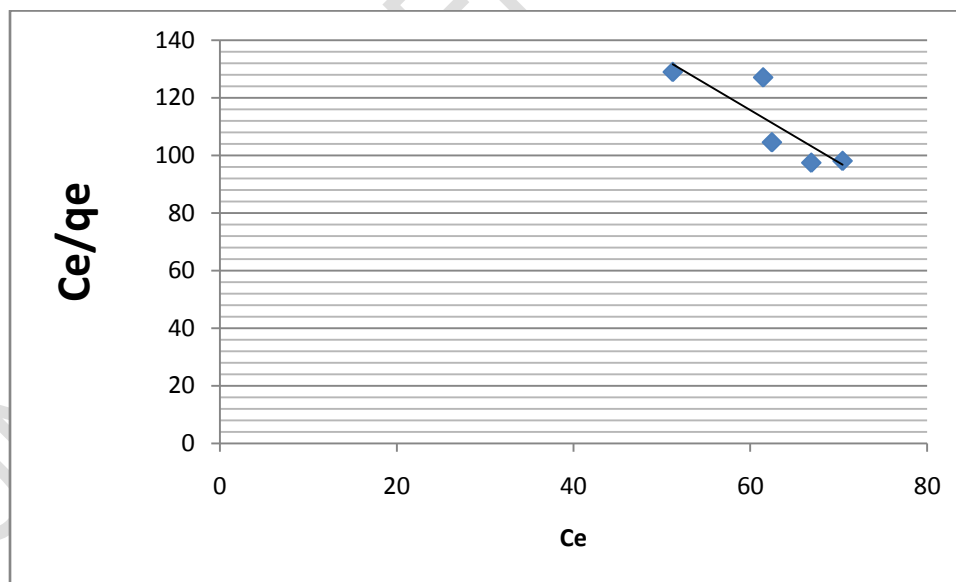


Fig 6: Langmuir isotherm plot for adsorption of Enyigba on SSM

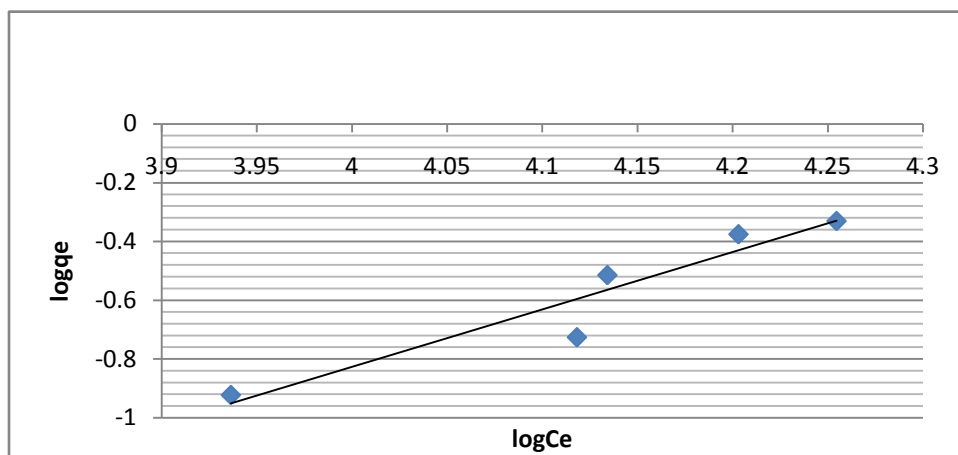


Fig 7: Freundlich isotherm plot for adsorption of Enyigba on SSM

4.13 Kinetic studies

The first and second order kinetics model plots for adsorption are shown in figs 8 and 9, while the kinetic parameters are shown in tables 8. R^2 value was used to test for the fitness., the value was higher in 2nd order than in 1st order.; a show of good linearity. It follows that the adsorption was best described as a 2nd order kinetic process. Moreover, a look at the theoretical q_e and adsorption rate constant k , were much higher in 2nd order than in 1st order, a further indication of the fitness of experimental data into the 2nd order kinetic model [24]. The mechanistics of adsorption was determined, utilizing the intra-particle diffusion model. The adsorption of Enyigba was not linear during the entire process; even the linear portion of the curve did not pass through the origin indicating that the intra-particle diffusion was not the only rate controlling step. It can be seen that there are two distinct regions—the initial pore diffusion due to external mass transfer effects with slope of 0.0044; followed by the intra-particle diffusion with slope of 0.493. The constant (k) for intra-particle diffusion was determined from the slope of the linear portion of the plot. R^2 value of 0.443, shows that the intra-particle diffusion can only account for 44.3% of the adsorption of Enyigba. This indicates the mechanism of Enyigba adsorption by SSM is complex and both, the surface adsorption as well as intra-particle diffusion contribute to the rate determining step [25]

Table 8: First and second order model parameters

MODEL	R^2	k	q_e
First Order	0.917	0.00001	0.5444
Second order	0.9624	0.0253	1.218
IPD*	0.443	0.493	0.234

IPD*- Intra Particle diffusion

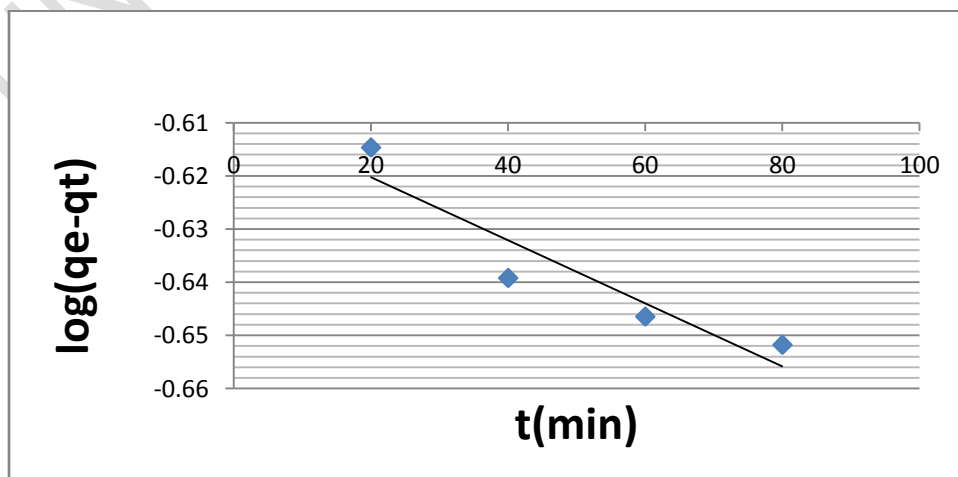


Fig 8: Pseudo-first order plot for adsorption of Enyigba on SSM

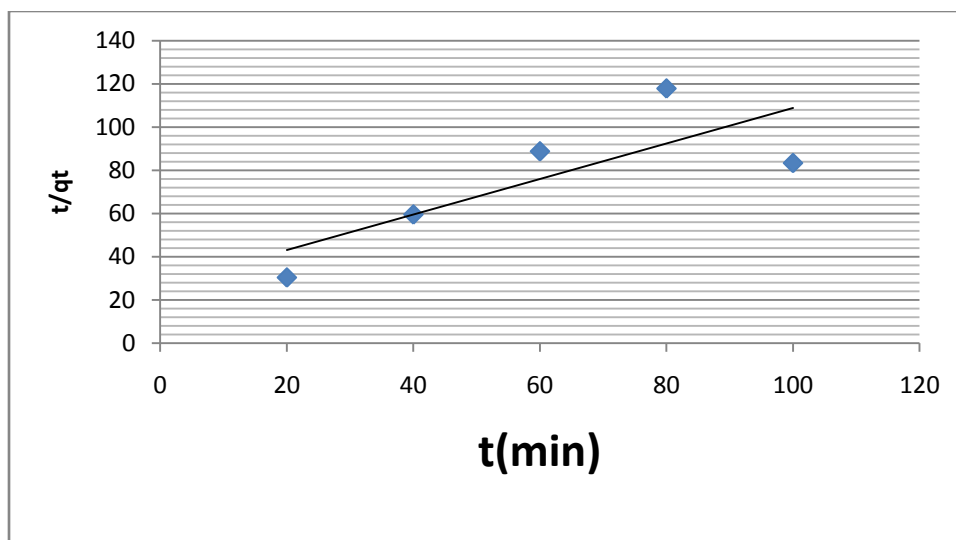


Fig 9: Pseudo-second order plot for adsorption of Enyigba on SSM

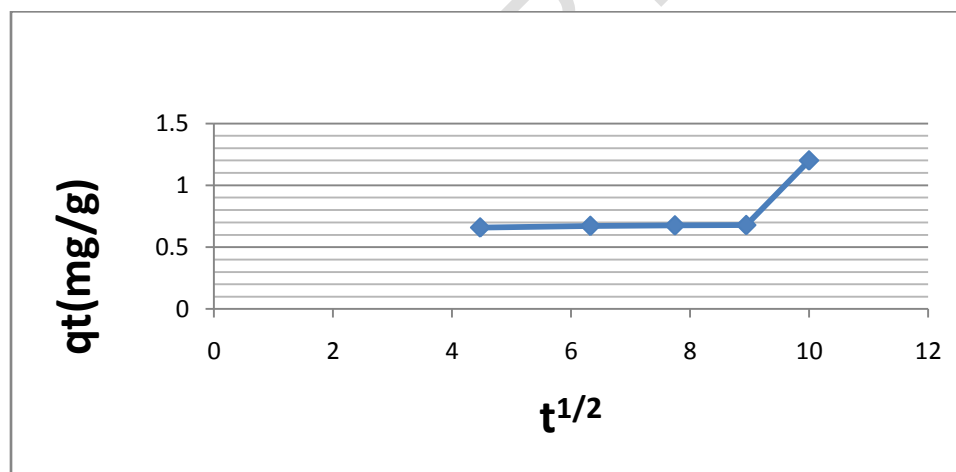


Fig 10: Intraparticle diffusion plot for adsorption of Enyigba on SSM

4.14 Thermodynamics

The thermodynamic parameters for the adsorption process were calculated by the following equations:

$$\Delta G^{\circ} = \Delta H^{\circ} - T\Delta S^{\circ} \quad 16$$

$$\Delta G^{\circ} = -RT \ln K_c \quad 17$$

$$\ln K_c = \frac{\Delta S^{\circ}}{R} - \frac{\Delta H^{\circ}}{RT} \quad 18$$

where, ΔG° is the Gibbs free energy, ΔH° is standard enthalpy (kJ mol^{-1}), ΔS° is standard entropy (kJ mol^{-1}), T is the absolute temperature (K), R is the gas constant ($8.314 \text{ J mol}^{-1} \text{ K}^{-1}$) and K_c is the distribution coefficient (L g^{-1}). The experiments were conducted at 293, 313, 333, 353 and 373 K. The values of ΔH° and ΔS° were determined from the slope and intercept of the plot of $\ln K_c$ vs. $1/T$ (Fig. 11). ΔG° was also calculated using Eq. 17.

The values of the thermodynamic parameters for the adsorption of Enyigba on SSM are shown in Table 9. The positive value of ΔH° for the process signifies the endothermic nature of the process. When the value of ΔH° is lower than 40 kJ mol^{-1} , it can be concluded that the adsorption process is physical. Obtained ΔH° value is $11.05 \text{ kJ mol}^{-1}$ showing that the adsorption process was physical in nature with weak Van der waals forces of attraction [26], which is consistent with the results of the isotherm model. The positive value of ΔS° reflects the affinity of the adsorbent material toward Enyigba and

the negative value of ΔG° show that the adsorption process was spontaneous and more favourable at higher temperatures[27]

Table 9: Thermodynamic parameters for the adsorption of Enyigba
T(K)

T(K)	$\Delta G(\text{kJ/mol})$	ΔH (kJ/mol)	ΔS (J/mol/K)
293	0.1827	11.0515	37.0948
313	-0.5592		
333	-1.3011		
353	-2.0430		
373	-2.7849		

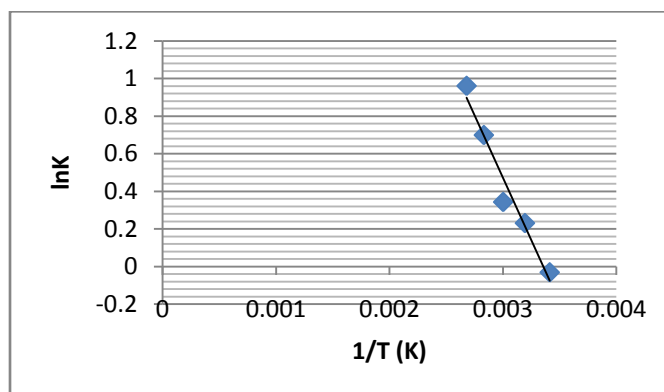


Fig 11: Thermodynamic plot of Enyigba onto SSM

After adsorption, Pb^{2+} was undetected in the Enyigba River water sample, which implies that the adsorbent was effective in removing the ions.

4. CONCLUSION

The Enyigba River is slightly polluted with Enyigba. The adsorbent was able to remove Enyigba from the aqueous solution. The FTIR spectra of all the adsorbents revealed the presence of active functional groups responsible for binding of metal ions from the aqueous solution. The SEM morphology of the adsorbents revealed a porous surface which is desirable for efficient sorption of metal ions. RSM and ANN predicted the % removal of Enyigba well. The predicted response was very similar to the experimental response in the three adsorbents, this shows the importance of designing an experiment. The regression model equation showed that adsorption had indirect effect mostly with the linear factors but had direct effect either by quadratic or interactive effect of the factors. The pseudo-second order model presented the best fit to the adsorption process compared to the pseudo-first order and intraparticle diffusion

REFERENCES

1. Orij, John N., *Political Organization in Nigeria Since the Last Stone Age: A History of the Igbo People*. (2011). New York, NY: Palgrave Macmillan. ISBN 978-0-230-62193-0. LCCN 2010025628.
2. Okolo, C.C., Oyedotun, T.D.T., Akamigbo, F.O.R. Open cast mining: threat to water quality in rural community of Enyigba in south-eastern Nigeria. *Applied Water Science*, (2018), 8:204
3. Bagherpour, R., Tudeschi, H. Material handling in world-wide surface mines. *Aggregate International*, (2007), 5:10-14.
4. Ezeaku, P.I. Evaluating the influence of open cast mining of solid minerals on soil, land use and livelihood systems in selected areas of Nassarawa State, north-central Nigeria. *Journal Ecology Natural Environment*, (2012), 4(3): 62-70.

5. Okolo, C.C., Akamigbo, F.R.O., Ezeaku, P.I., Nwite, J.N., Nwatie, J.C., Ezeudo, V.C., Ene, J., Ukaegbu, E.P., Udegbonam, O.N., Eze, N.C. Impact of open cast mine land use on soil physical properties in Enyigba, South-eastern Nigeria and the implication for sustainable land use management. *Nigerian Journal of Soil Science*, (2015), 25(1):95-101
6. Aref, W., Ahmed, A., Mohd, S.H. Removing Heavy Metals through Different Types of Soils and Marble Powder found in Oman. *Journal of Ecological Engineering*. (2019), 20(4): 136–142. <https://doi.org/10.12911/22998993/102798>
7. Inyang, M., Gao B., Yao Y., Xue Y., Zimmerman A.R., Pullammanappallil P., Cao X. Removal of heavy metals from aqueous solution by biochars derived from anaerobically digested biomass. *Bioresource Technology*, (2012), 110: 50-56. DOI: [10.1016/j.biortech.2012.01.072](https://doi.org/10.1016/j.biortech.2012.01.072)
8. Nurzulaifa, S.E.M.Y., Zitty, S.I., Suhanom, M.Z., Mohd., F.A.A. (2016). Adsorption of Cu, As, Pb and Zn by Banana Trunk. *Malaysian Journal of Analytical Sciences*, (2012), 20(1): 187 – 196.
9. Gunatilake, S.K. Methods of removing heavy metals from industrial wastewater. *Methods*, (2015), 1(1):50-56.
10. www.ibm.com/docs/en/spss-statistics/25.0.0?topic=perceptron-training-multilayer (Accessed 17/07/2023)
11. Langmuir, I., The constitution and fundamental properties of solids and liquids, *Journal of American Society*. (1916), 38 (11): 2221 – 2295.
12. Freundlich, H.M.F., Ueber die Adsorption in Lösungen. *Zeitschrift für physikalische Chemie*. (1906), 57:385-470. In German
13. Ho YS, McKay G, Wase DAJ, Foster CF Study of the sorption of divalent metal ions on to peat. *Ads. Sci. Technol.* (2000), 18, 639–650.
14. Cheung WH, Szeto YS, McKay G. Intraparticle diffusion processes during acid dye adsorption onto chitosan. *Bioresources Technologies*, (2007), 98:2897–2904
15. <https://www.lenntech.com/who-eu-water-standards.htm#ixzz87tjTDrHZ>. (Accessed 17/07/2023)
16. Chakravarty, P., Sarma, N.S., and Sarma, H.P., Biosorption of cadmium (II) from aqueous solution using heart wood powder of *Areca catechu*. *Chemical Engineering Journal*. (2010), 162: 949-955
17. Akpomie, K.G., Dawodu, F.A. Treatment of an automobile effluent from heavy metals contamination by an eco-friendly montmorillonite. *Journal of Advanced Research*. (2015).6(6): 1003-1013
18. Xu Y, Axe L Synthesis and characterization of iron oxide-coated silica and its effect on metal adsorption. *J Colloid Interface Sci.* (2005), 282:11–19
19. Akpomie, K.G., Dawodu, F.A. Acid-modified montmorillonite for sorption of heavy metals from automobile effluent. *Journal of Basic and Applied Sciences*, (2016). 5(1) : 1-12
20. Ahmad, M.A. and Alrozi, R. Optimization of Preparation Conditions for Mangosteen Peel-Based Activated Carbons for the Removal of Remazol Brilliant Blue R Using Response Surface Methodology. *Chemical Engineering Journal*, (2010), 165 : 883-890. <https://doi.org/10.1016/j.cej.2010.10.049>.
21. Garba Z. N., Afidah A. R., Process optimization of $K_2C_2O_4^-$ activated carbon from *Prosopis africana* seed hulls using response surface methodology, *J. Anal. Appl. Pyrol.*, (2014)107:306-312.
22. Menkiti M. C., Aniagor C. O., Parametric Studies on Descriptive Isotherms for the Uptake of Crystal Violet Dye from Aqueous Solution onto Lignin-Rich Arab J Sci Eng DOI 10.1007/s13369-017-2789-3
23. Naiya T. K., Chowdhury P., Bhattacharya A. K., Das S. K., Saw dust and neem bark as low-cost natural biosorbent for adsorptive removal of Zn(II) and Cd(II) ions from aqueous solutions, *Chemical Engineering Journal*, (2009), 148:1,68-79
24. Egwuatu C. I., Iloamaeke I., Anarado C. J. O., Umeohia O. C., Locally-Sourced Beans Husk, a Potential Adsorbent for Cd(II), Pb(II), Hg(II) Ions in Aqueous Solution, *International Journal of Science and Research* (2015) 4:8, 1129-1137
25. Srivastava V.C., Swamy M.M., Mall I.D., Prasad B., Mishra I.M., Adsorptive removal of phenol by bagasse fly ash and activated carbon: equilibrium, kinetics and thermodynamics, *Colloids Surf. A: Physicochem. Eng. Aspects*, (2006) 272:89–104.
26. De Luna, M.D.G., C.M. Futralan, C.A. Jurado, J.I. Colades and M.W. Wan., Removal of ammonium nitrogen from aqueous solution using chitosan coated bentonite: Mechanism and effect of operating parameters. *J. Applied Polym. Sci.*, 2017. DOI: [10.1002/app.45924](https://doi.org/10.1002/app.45924).
27. Gok, C., U. Gerstmann and S. Aytas, Biosorption of radiostrontium by alginate beads: Application of isotherm models and thermodynamic studies. *J. Radioanal. Nucl. Chem.*, (2013). 295: 777-788

UNDER PEER REVIEW